J|A|C|S
ARTICLES
Published on Web 02/04/2004

Design, Synthesis, and Crystallographic Studies of Neutral Platinum-Based Macrocycles Formed via Self-Assembly

Partha Sarathi Mukherjee,* Neeladri Das, Yury K. Kryschenko, Atta M. Arif, and Peter J. Stang*

Contribution from the Department of Chemistry, University of Utah, 315 South 1400 East, Room 2020, Salt Lake City, Utah 84112

Received October 25, 2003; E-mail: stang@chem.utah.edu

Abstract: A series of neutral, platinum-based macrocycles was synthesized from rigid oxygen donor building blocks via self-assembly. The combination of a platinum-based 60° acceptor unit **1** with several linear and angular dicarboxylate bridging ligands afforded hitherto unknown neutral platinum-based supramolecular triangles and rhomboids. In addition, a similar reaction of the diplatinum molecular clip **6** and three different linear dicarboxylates led to the formation of neutral molecular rectangles. Most of the macrocycles were characterized by X-ray single-crystal structure analysis, and, in all cases, NMR spectra were consistent with the formation of single highly symmetrical species.

Introduction

One of the growth areas at the forefront of modern supramolecular chemistry is the coordination-driven self-assembly of discrete molecular ensembles.[1] The interest in these species is fueled by their size- and shape-selective properties, with potential applications in catalysis and sensing devices.[1] The list of two-dimensional structures reported to date includes an array of supramolecular macrocycles,[2] ranging in complexity from simple triangular assemblies[3,4] to higher symmetry polygons such as hexagons.[2g]

Square-planar platinum and palladium have long been among the favorite metals in the area of coordination-driven self-assembly. Yet, interestingly, all of the self-assembled structures that include these metals used neutral nitrogen-based linkers as the donor units in the self-assembly processes.[1a−b,f,g] As a result, the supramolecular structures formed are positively charged. This makes such assemblies hosts for electron-rich species. Assemblies without charge, which are expected to be more suitable for encapsulation of neutral organic guests, have also been reported. These species are based upon coordination of anionic ligands to other metals, such as Mo,[5] Rh,[5b,6] Re,[7] and Zn.[7d−e] Until recently,[8a] oxygen-to-platinum coordination has not been used as the driving force in the construction of supramolecular self-assemblies, as complexes incorporating

(1) (a) Seidel, S. R.; Stang, P. J. *Acc. Chem. Res.* **2002**, *35*, 972. (b) Swiegers, G. F.; Malefetse, T. J. *Coord. Chem. Rev.* **2002**, *225*, 91. (c) Holliday, B. J.; Mirkin, C. A. *Angew. Chem., Int. Ed.* **2001**, *40*, 2022. (d) Cotton, F. A.; Lin, C.; Murillo, C. A. *Acc. Chem. Res.* **2001**, *34*, 759. (e) Fujita, M.; Umemoto, K.; Yoshizawa, M.; Fujita, N.; Kusukawa, T.; Biradha, K. *Chem. Commun*. **2001**, 509. (f) Leininger, S.; Olenyuk, B.; Stang, P. J. *Chem. Rev.* **2000**, *100*, 853. (g) Uller, E.; Demleitner, I.; Bernt, I.; Saalfrank, R. W. Synergistic Effect of Serendipity and Rational Design in Supramolecular Chemistry. In *Structure and Bonding*; Fujita, M., Ed.; Springer: Berlin, 2000; Vol. 96, p 149. (h) Caulder, D. L.; Raymond, K. N. *J. Chem. Soc., Dalton Trans.* **1999**, 1185. (i) Caulder, D. L.; Raymond, K. N. *Acc. Chem. Res.* **1999**, *32*, 975. (j) Baxter, P. N. W.; Lehn, J.-M.; Baum, G.; Fenske, D. *Chem.-Eur. J.* **1999**, *5*, 102. (k) Fujita, M. *Chem. Soc. Rev.* **1998**, *27*, 417. (l) Chambron, J.-C.; Dietrich-Buchecker, C.; Sauvage, J.-P. Transition Metals as Assembling and Templating Species. In *Comprehensive Supramolecular Chemistry*; Lehn, J.-M., Chair, E., Atwood, J. L., Davis, J. E. D., MacNicol, D. D., Vogtle, F., Eds.; Pergamon Press: Oxford, 1996; Vol. 9, Chapter 2, p 43. (m) Lehn, J.-M. *Supramolecular Chemistry: concepts and perspectives*; VCH: New York, 1995.

(2) (a) Pak, J. J.; Greaves, J.; McCord, D. J.; Shea, K. J. *Organometallics* **2002**, *21*, 3552. (b) Lee, S. J.; Lin, W. *J. Am. Chem. Soc.* **2002**, *124*, 4554. (c) Liu, X.; Stern, C. L.; Mirkin, C. A. *Organometallics* **2002**, *21*, 1017. (d) Han, G.; Dong, G.; Duan, C.-Y.; Mo, H.; Meng, Q.-J. *New J. Chem.* **2002**, *26*, 1371. (e) Sun, S.-S.; Anspach, J. A.; Lees, A. J. *Inorg. Chem.* **2002**, *41*, 1862. (f) Manimaran, B.; Thanasekaran, P.; Rajendran, T.; Lin, R.-J.; Chang, I.-J.; Lee, G.-H.; Peng, S.-M.; Rajagopal, S.; Lu, K.-L. *Inorg. Chem.* **2002**, *41*, 5323. (g) Abourahma, H.; Moulton, B.; Kravtsov, V.; Zaworotko, M. J. *J. Am. Chem. Soc.* **2002**, *124*, 9990. (h) Cui, Y.; Ngo, H. L.; Lin, W. *Inorg. Chem.* **2002**, *41*, 1033. (i) Cotton, F. A.; Lin, C.; Murillo, C. A. *J. Am. Chem. Soc.* **2001**, *123*, 2670. (j) Cotton, F. A.; Daniels, L. M.; Lin, C.; Murillo, C. A.; Yu, S.-Y. *J. Chem. Soc., Dalton Trans.* **2001**, 502. (k) Kuehl, C. J.; Huang, S. D.; Stang, P. J. *J. Am. Chem. Soc.* **2001**, *123*, 9634. (l) Campos-Fernandez, C. S.; Clerac, R.; Koomen, J. M.; Russell, D. H.; Dunbar, K. R. *J. Am. Chem. Soc.* **2001**, *123*, 773. (m) Kuehl, C. J.; Mayne, C. L.; Arif, A. M.; Stang, P. J. *Org. Lett.* **2000**, *2*, 3727. (n) Schmitz, M.; Leininger, S.; Fan, J.; Arif, A. M.; Stang, P. J. *Organometallics* **1999**, *18*, 4817. (o) Habicher, T.; Nierengarten, J.-F.; Gramlich, V.; Diederich, F. *Angew. Chem., Int. Ed.* **1998**, *37*, 1916. (p) Stang, P. J.; Persky, N. E.; Manna, J. *J. Am. Chem. Soc.* **1997**, *119*, 4777. (q) Hartshorn, C. M.; Steel, P. J. *Inorg. Chem.* **1996**, *35*, 6902.

(3) (a) Qin, Z.; Jennings, M. C.; Puddephatt, R. J. *Inorg. Chem.* **2002**, *41*, 3967 (b) Qin, Z.; Jennings, M. C.; Puddephatt, R. J. *Chem. Commun.* **2001**, 2676. (c) Schweiger, M.; Seidel, S. R.; Arif, A. M.; Stang, P. J. *Angew. Chem., Int. Ed.* **2001**, *40*, 3467. (d) Sun, S.-S.; Lees, A. J. *Inorg. Chem.* **1999**, *38*, 4181. (e) Cotton, F. A.; Lin, C.; Murillo, C. A. *Inorg. Chem.* **2001**, *40*, 575.

(4) Kryschenko, Y. K.; Seidel, S. R.; Arif, A. M.; Stang, P. J. *J. Am. Chem. Soc.* **2003**, *125*, 5193.

(5) (a) Cotton, F. A.; Donahue, J. P.; Murillo, C. A. *J. Am. Chem. Soc.* **2003**, *125*, 5436. (b) Cotton, F. A.; Lin, C.; Murillo, C. A. *Inorg. Chem.* **2001**, *40*, 478. (c) Cotton, F. A.; Lin, C.; Murillo, C. A. *Inorg. Chem.* **2001**, *40*, 6413. (d) Cheng, H.; Chun-Ying, D.; Chen-jie, F.; Yong-jiang, L.; Qing-jin, M. *J. Chem. Soc., Dalton Trans.* **2000**, 1207. (e) Cotton, F. A.; Daniels, L. M.; Lin, C.; Murillo, C. A. *J. Am. Chem. Soc.* **1999**, *121*, 4538.

(6) Cotton, F. A.; Lin, C.; Daniels, M. L.; Murillo, C. A.; Yu, S.-Y. *J. Chem. Soc., Dalton Trans.* **2001**, 502.

(7) (a) Bala, M.; Thanasekaran, P.; Rajendran, T.; Liao, R. T.; Liu, Y. H.; Lee, G. H.; Peng, S. M.; Rajagopal, S.; Lu, K. L. *Inorg. Chem.* **2003**, *42*, 4795. (b) Manimaran, B.; Rajendran, T.; Lu, Y. L.; Lee, G. H.; Peng, S. M.; Lu, K. L. *Eur. J. Inorg. Chem.* **2001**, *3*, 633. (c) Slone, R. V.; Hupp, J. T.; Albrecht-Schmitt, T. E. *Inorg. Chem.* **1996**, *35*, 4096. (d) Saalfrank, R. W.; Reimann, U.; Goritz, M.; Hampel, E.; Scheurer, A.; Heinemann, F. W.; Busches, M.; Daub, J.; Schunemann, V.; Trautwein, A. X. *Chem.-Eur. J.* **2002**, *8*, 3614. (e) Saalfrank, R. W.; Trummer, S.; Reimann, U.; Chowdhry, M. M.; Hampel, F.; Waldmann, O. *Angew. Chem., Int. Ed.* **2000**, *39*, 3492.

10.1021/ja039235b CCC: $27.50

Scheme 1. Self-Assembly of Neutral Pt-Based Macrocycles

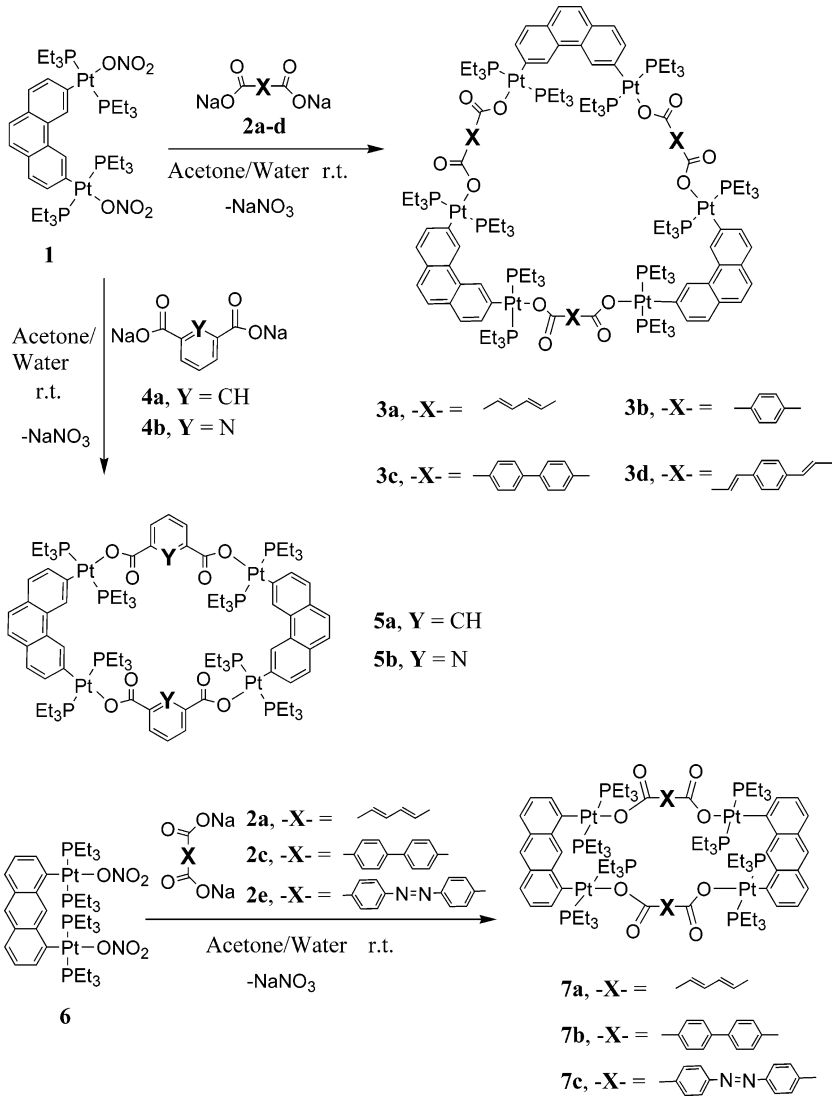

platinum−oxygen bonds were believed to be unstable due to the weak bonding between a hard ligand and a soft metal.[8b]

Here, we report the design, self-assembly, and characterization of a series of platinum(II)-based neutral supramolecular macrocycles, such as molecular triangles and rhomboids. Both kinds of macrocycles use 60° Pt(II)-based building block[4] **1** as an acceptor unit, and ditopic angular (in the case of rhomboids) or linear (in the case of triangles) dicarboxylate bridging ligands. Selected linear dicarboxylate anions also provided neutral supramolecular rectangles in combination with the diplatinum molecular clip **6**. Characterization of these new macrocycles by X-ray crystallography, multinuclear NMR, and infrared spectroscopy is discussed along with selected properties.

Results and Discussion

Self-Assembly and Spectral Studies. The neutral supramolecular triangles, rhomboids, and rectangles were assembled as shown in Scheme 1. Addition of an aqueous solution of the linear linkers **2a**−**d**, respectively, to an acetone solution, containing 1 equiv of the 60° platinum acceptor linker **1**, resulted in immediate precipitation of the neutral triangular macrocycles **3a**−**d**, respectively, in 97−99% isolated yield. Similar treatment of **1** with aqueous solutions of the 120° angular linkers **4a** and **4b** produced the supramolecular rhomboids **5a** and **5b** as white solids also in 97−99% isolated yield. In a similar manner, supramolecular rectangles **7b** and **7c** are formed instantly as aqueous solutions of dicarboxylates **2c** and **2e** are added to the diplatinum clip **6**, dissolved in acetone. In contrast to other neutral platinum-based macrocyclic structures, rectangle **7a** requires stirring an equimolar mixture of **2a** and **6** in aqueous acetone for 12 h for self-assembly to be completed.

The ^{31}P NMR spectra of macrocycles **3a**−**d**, **5a**, **5b**, and **7a**−**c** are in all cases consistent with the formation of a single, highly symmetrical species, as indicated by the appearance of sharp singlets with concomitant ^{195}Pt satellites. For triangles **3a**−**d** and rhomboids **5a** and **5b**, this singlet appears around 17.5 ppm and is shifted approximately 2.5 ppm upfield relative to its position in precursor **1**. In the case of rectangles **7a**−**c**, the ^{31}P signal is located around 13 ppm, with an upfield shift of 1 ppm or less as compared to the position of precursor **6**. The small change in the position of the phosphorus signal in comparison to that of the starting materials (**1** or **6**) can be attributed to the close similarity between the newly formed

(8) (a) Das, N.; Mukherjee, P. S.; Arif, A. M.; Stang, P. J. *J. Am. Chem. Soc.* **2003**, *125*, 13950. (b) Greenwood, N. N.; Earnshaw, A. *Chemistry of the Elements*; Pergamon: Oxford, 1984.

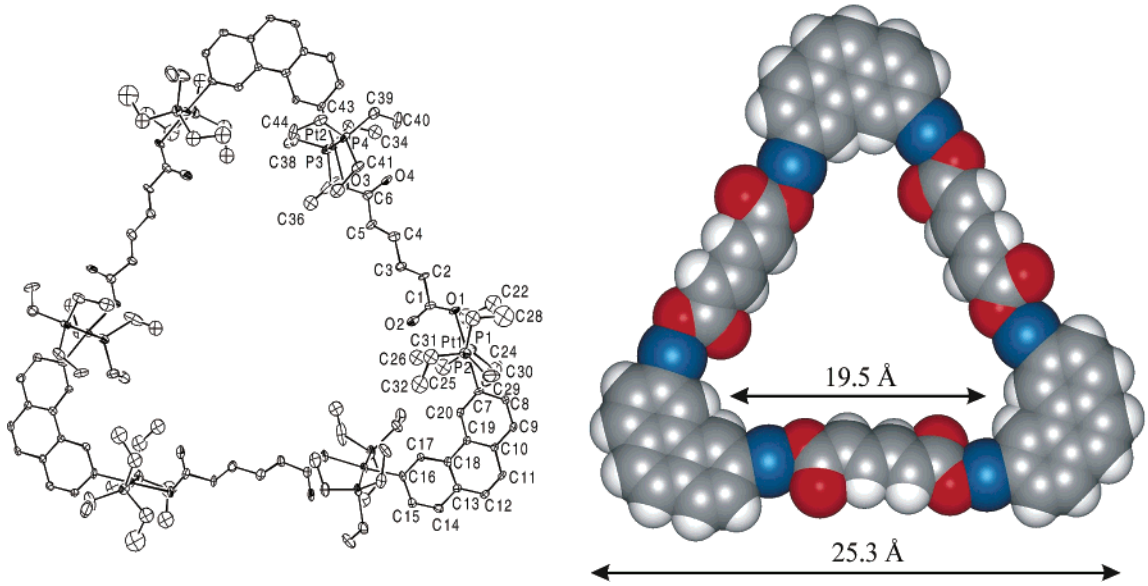

Figure 1. ORTEP presentation with atom numbering scheme of **3a** (left), and CPK model showing inner and outer dimensions of **3a** (right).

Table 1. Crystallographic Data and Refinement Parameters for **3a**, **3b**, **5a**, and **5b**

	3a	3b	5a	5b
formula	$C_{132}H_{234}P_{12}O_{21}Pt_6$	$C_{140}H_{218}Cl_6P_{12}O_{12}Pt_6$	$C_{95}H_{147}Cl_9P_8O_8Pt_4$	$C_{90}H_{146}N_2P_8O_{10}Pt_4$
fw	3699.37	3848.02	2764.30	2444.21
temp (K)	150(1)	150(1)	150(1)	150(1)
λ (Å)	0.71073	0.71073	0.71073	0.71073
crystal system	hexagonal	hexagonal	monoclinic	orthorhombic
space group	$P6_3$	$P6_3$	$C2$	P_{bca}
a (Å)	26.416(5)	26.231(9)	65.852(13)	17.296(2)
b (Å)	26.416(5)	26.231(9)	13.947(3)	21.745(5)
c (Å)	12.1562(9)	14.506(5)	18.509(4)	26.395(3)
α (deg)	90	90	90	90
β (deg)	90	90	96.533(8)	90
γ (deg)	120	120	90	90
V (Å^3)	8225.2(3)	8644.1(5)	16 820.2(6)	9927.81(19)
Z	2	2	6	4
D_{calc} (g/cm^3)	1.494	1.478	1.637	1.635
μ (mm^{-1})	5.254	5.088	5.325	5.801
F(000)	3684	3808	8196	4848
reflns collected	23 892	17 624	33 677	21 759
unique reflns	12 322	9542	33 677	11 334
max and min trans	0.4197, 0.2277	0.4611, 0.3627	0.4141, 0.2356	0.3249, 0.2360
R1 [$I > 2\sigma(I)$][a]	0.0576	0.0705	0.0443	0.0286
wR2	0.1371	0.1679	0.1012	0.0603

[a] $R1 = (F_o - F_c)/F_o$, $wR2 = [(w(F_o^2 - F_c^2)^2)/(F_o^2)^2]^{1/2}$.

platinum−oxygen bond and the Pt−ONO_2 bond in the starting materials.

The ^{1}H NMR spectra of these neutral macrocycles are also indicative of highly symmetrical structures and display significant spectroscopic differences from the precursor building blocks, as well as from their previously reported charged counterparts.[4]

In the IR spectra of all of the macrocycles, absorptions arising from the corresponding dicarboxylates were observed. The carbonyl stretching frequency of the starting **2a** and **2c** appeared at 1620 and 1590 cm^{-1}, respectively, whereas the corresponding macrocycles **3a** and **3c** showed the carbonyl absorption at 1638 and 1619 cm^{-1}. Similar shifts to higher wavenumber also appeared in the other macrocycles, presumably due to the coordination to Pt.

Crystal Structure of Triangles 3a and 3b. X-ray crystallography unambiguously established the structure of the neutral triangles **3a** and **3b**. The molecular structure of **3a** is shown in Figure 1. Crystallographic data and refinement parameters are given in Table 1. The exterior length of triangle **3a** is approximately 25.3 Å, while the internal cavity measures approximately 19.5 Å. The geometry around each Pt is close to square planar with an O(1)−Pt(1)−P(1) angle of 87.50(4)°, an O(1)−Pt(1)−P(2) angle of 91.20(4)°, and a P(1)−Pt(1)−P(2) angle of 177.7(14)°. Especially interesting is the packing pattern of this complex in the solid state. The triangles are packed in layers, which form long channels of triangular shape of approximately 16.5 Å diameter as shown in Figure 2. The stacking of the neighboring triangles produces smaller hexagonal channels of diameter 11.1 Å. Both the triangular and the hexagonal channels are hydrophilic and occupied by water molecules. Characteristic bond parameters are given in Table 2. The repeating unit distance between each stacked neutral triangle is 15.6 Å, which is similar to that of the cationic triangle reported previously.[3a]

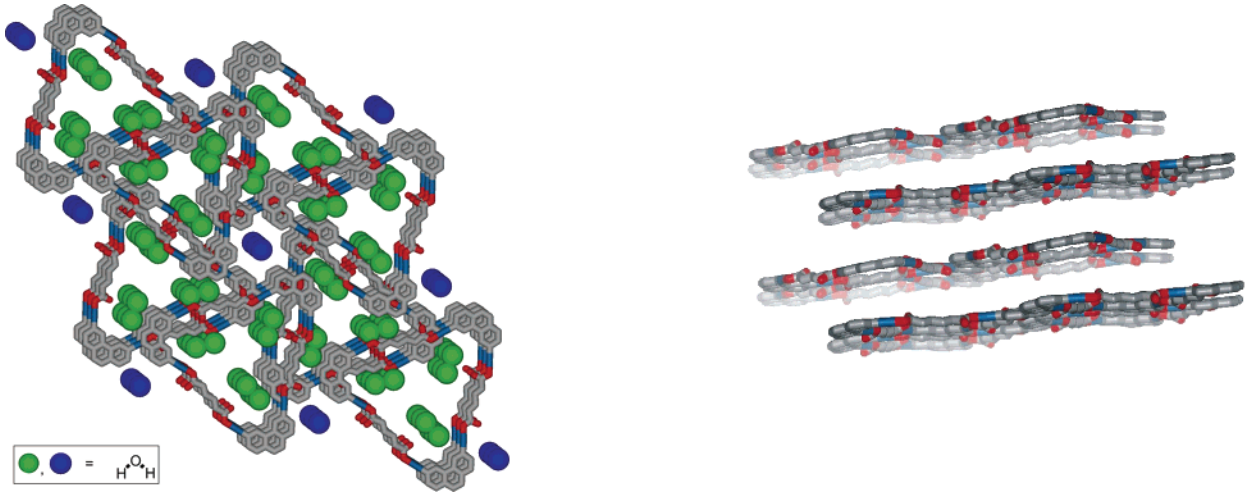

Figure 2. Packing diagram of **3a** along the *c* axis (left); solvents in the triangular channels are shown in green, while solvents in the hexagonal channels are shown in blue (CPK). Side view of the stacking nature of different sheets (right).

Table 2. Selected Bond Lengths (Å) and Angles (deg) for Complexes **3a**, **3b**, **5a**, and **5b**

3a

Pt(1)−O(1)	2.125(6)	Pt(1)−P(1)	2.304(6)	Pt(1)−P(2)	2.311(5)
Pt(2)−O(3)	2.115(6)	Pt(2)−P(3)	2.287(3)	Pt(2)−P(4)	2.299(3)

O(1)−Pt(1)−P(1)	87.50(4)	O(1)−Pt(1)−P(2)	91.20(4)
P(1)−Pt(1)−P(2)	177.7(14)	O(3)−Pt(2)−P(4)	91.10(3)
O(3)−Pt(2)−P(3)	92.10(3)	P(3)−Pt(2)−P(4)	172.6(15)

3b

Pt(1)−O(1)	2.117(10)	Pt(1)−P(1)	2.311(7)	Pt(1)−P(2)	2.197(11)
Pt(2)−O(3)#1	2.124(11)	Pt(2)−P(3)	2.290(7)	Pt(2)−P(4)	2.266(7)

O(1)−Pt(1)−P(1)	91.70(5)	O(1)−Pt(1)−P(2)	89.20(5)
P(1)−Pt(1)−P(2)	175.1(2)	O(3)#1−Pt(2)−P(4)	93.8(5)
O(3)#1−Pt(2)−P(3)	87.40(5)	P(3)−Pt(2)−P(4)	177.3(4)

5a

Pt(1)−O(1)	2.112(6)	Pt(1)−P(1)	2.302(3)	Pt(1)−P(2)	2.262(3)
Pt(2)−O(7)	2.125(5)	Pt(2)−P(8)	2.291(5)	Pt(2)−P(7)	2.292(3)
Pt(3)−O(5)	2.120(5)	Pt(3)−P(5)	2.303(3)	Pt(4)−O(3)	2.117(5)

Pt(4)−P(4)	2.287(3)	Pt(4)−P(3)	2.310(3)
O(1)−Pt(1)−P(1)	91.10(2)	O(1)−Pt(1)−P(2)	87.00(2)
P(1)−Pt(1)−P(2)	177.9(10)	O(7)−Pt(2)−P(7)	92.20(2)
O(5)−Pt(3)−P(6)	91.40(2)	P(3)−Pt(4)−P(4)	178.57(10)

5b

Pt(1)−O(1)	2.149(2)	Pt(1)−P(1)	2.291(10)	Pt(1)−P(2)	2.277(11)
Pt(2)−O(3)	2.129(2)	Pt(2)−P(3)	2.294(10)	Pt(2)−P(4)	2.293(10)

O(1)−Pt(1)−P(1)	88.11(8)	O(1)−Pt(1)−P(2)	91.55(8)
P(1)−Pt(1)−P(2)	167.49(4)	O(3)−Pt(2)−P(4)	84.93(8)
O(3)−Pt(2)−P(3)	93.87(8)	P(3)−Pt(2)−P(4)	175.19(4)

Complex **3b** is isostructural with **3a** (Figure 3), and the asymmetric unit contains one-third of the assembly accompanied by two chloroform molecules; the triangles are packed in layers which are packed as shown in Figure 3. In this case, no ordered channel structure is evident (cf., **3a**). The distance between the centroid of the benzene ring of terephthalate and that of the middle benzene ring of the phenanthroline moiety is 20.4 Å. The interlayer Pt−Pt distance in **3b** is 10.0 Å. The internal cavity size is 20.9 Å, while the outer dimension is 24.6 Å (as measured between the innermost and outermost hydrogens). The geometry around each Pt in **3b** is close to square planar. Selected bond lengths and angles are presented in Table 2.

Attempts to obtain good quality single crystals of **3c** failed. Nevertheless, the cell parameters, crystal system [*a*, 30.884(6); *b*, 30.884(6); *c*, 13.781(3) Å; α, 90°; *β*, 90°; *γ*, 120°; hexagonal; space group, $P6_3$; *Z*, 2; *V*, 11 384.38(40) Å^3], and NMR data are consistent with those of the triangles **3a** and **3b**.

Crystal Structure of the Rhomboids 5a and 5b. Diffraction quality single crystals of **5a** and **5b** were grown overnight by vapor diffusion of acetone into a chloroform/dichloromethane solution of each individual complex. The important crystallographic parameters of these complexes are given in Table 1. The Pt−P and Pt−O (see Table 2) bond lengths are in the expected range.[9−12] These are the first examples of neutral nanoscopic molecular rhomboids derived from any metal containing a 60° corner unit (Figures 4 and 5). The geometry around the Pt(II) center in both of these complexes is square planar (Table 2). The bridging of the isophthalate in **5a** is syn−anti, while in **5b** the dicarboxylate is linked in a syn−syn fashion. The dimensions of rhomboid **5a** are 15.1 × 11.8 Å, as measured by intraring Pt(1)−Pt(3) and C(7)−C(29) distances. Similarly, the dimensions of **5b** are 15.1 × 13.0 Å. Complex **5a** crystallized with highly disordered chloroform inside the cavities, whereas **5b** is crystallized with water molecules. The presence of the inner-directed pyridine nitrogen makes the rhomboidal loop of **5b** more polar than that of **5a**. The water molecule in **5b** is hydrogen bonded to the carboxylate oxygen. The packing nature of these complexes is shown in Figures 4 and 5. In the solid state of **5a**, the rhomboids are packed in such a way that four neighboring macrocycles define a smaller rhomboidal ring. The resulting sheets are stacked on top of each other, forming two different types of rhomboidal channels (Figure 4). The larger channels are occupied by solvent molecules, whereas the smaller channels (approximate size 4.4 Å) are empty. The Pt−Pt distance between layers in **5a** is 13.9 Å. This distance is very close to that of some cationic rhomboids reported earlier.[2l,13−15] However, in the case of **5b**, analogous

(9) Whiteford, J. A.; Lu, C. V.; Stang, P. J. *J. Am. Chem. Soc.* **1997**, *119*, 2524.
(10) Stang, P. J.; Chen, K.; Arif, A. M. *J. Am. Chem. Soc.* **1995**, *117*, 8793.
(11) (a) Flint, B.; Li, J.-J.; Sharp, P. R. *Organometallics* **2002**, *21*, 997. (b) Klooster, W. T.; Voss, E. J. *Inorg. Chim. Acta*. **1999**, *285*, 10.
(12) (a) Andrews, M. A.; Gould, G. L.; Klooster, W. T.; Koeins, K. S.; Voss, E. J. *Inorg. Chem*. **1996**, *35*, 5478. (b) Andrews, M. A.; Voss, E. J.; Gould, G. L.; Klooster, W. T.; Koetzle, T. F. *J. Am. Chem. Soc.* **1994**, *116*, 5730.
(13) Fujita, M.; Aoyagi, M.; Ogura, K. *Inorg. Chim. Acta*. **1996**, *246*, 53.
(14) Habicher, T.; Nierengarten, J.-F.; Gramlich, V.; Diederich, F. *Angew. Chem., Int. Ed.* **1998**, *37*, 1917.
(15) Hartshorn, C. M.; Steel, P. J. *Inorg. Chem*. **1996**, *35*, 6902.

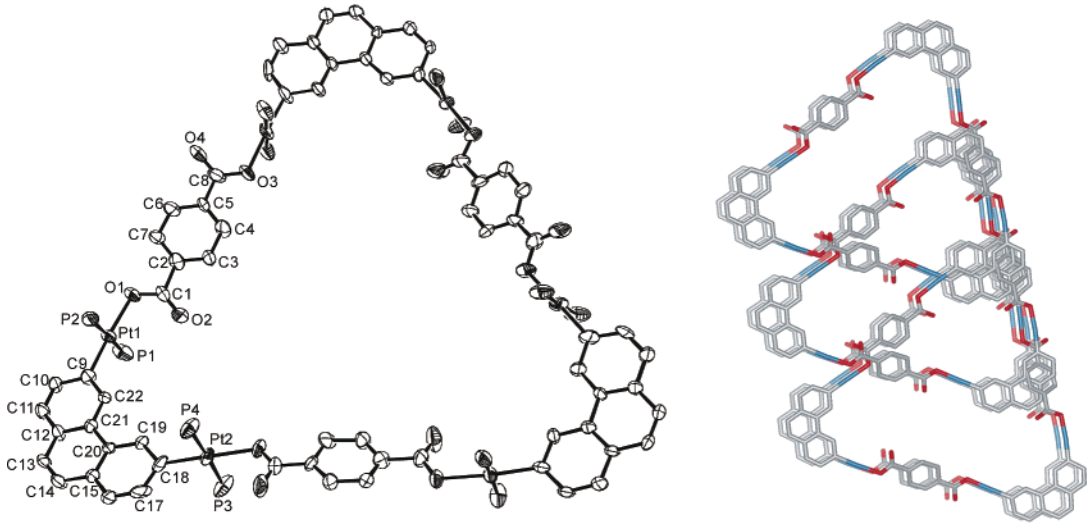

Figure 3. ORTEP of triangle **3b** with atom numbering (left). Packing nature of **3b**; triethylphosphine, hydrogen, and solvent molecules are omitted for clarity (right).

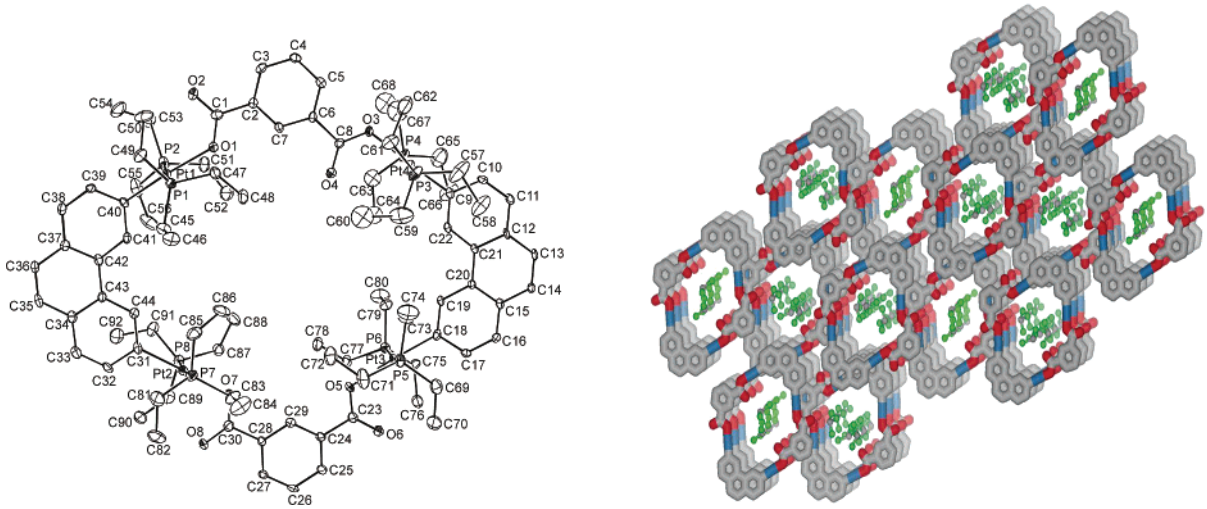

Figure 4. ORTEP presentation of **5a** with atom numbering (left). Packing diagram of **5a** along the *a* axis; disordered chloroform molecules in the channels are shown as ball-and-stick models (right).

channels are not found. This is due primarily to the orchestrated arrangement of the alternate rhomboids (Figure 5).

Crystal Structure of Rectangles 7a−c. The structures of the macrocycles **7a−c** were unambiguously determined by X-ray crystallography. Quality single crystals grew at ambient temperature by vapor diffusion of acetone into a concentrated $CHCl_3/CH_2Cl_2$ mixture of the corresponding complexes. The important crystallographic parameters for **7a−c** are given in Table 3. Selected bond parameters are cited in Table 4. Figure 6 shows the ORTEP presentation of **7a**. Similar to rhomboid **5b**, the dicarboxylate in **7a** is linked in a syn−syn fashion. The distortion of **6** affects the geometry of **7a** such that the bridging muconic acid ligands are forced to bend outward, which in turn causes the rectangle to appear bowed in the middle. This bending is due to the steric repulsion of the triethylphosphines that to a small extent pushes the platinum atoms apart. The length of **7a** is 15.5 Å. The width, as defined by the distance between the metals, is 5.40 Å, while the distance between the centroids of the ethylenic moieties is 7.72 Å. A top view of the packing is shown in Figure 6. All of the solvent molecules are situated outside of the rectangles in the pockets created by the triethylphosphine groups of different rectangles. The distance between two parallel rectangles is 13.3 Å. This packing is close to that of the previously reported cationic rectangles.[2j]

Similarly, the crystal structures of **7b** and **7c** show (Figures 7 and 8) rectangles with almost square-planar geometries around each Pt atom. Selected bond parameters are provided in Table 4. The bridging dicarboxylates in both of these complexes are again linked in a syn−syn fashion. The approximate lengths of **7b** and **7c** are 19.5 and 21.5 Å, respectively. The width, as defined by the Pt atoms, is 5.43 Å (**7b**) and 5.33 Å (**7c**). The distance between the inner nitrogens in **7c** is 6.19 Å. These structures are also slightly bowed in the middle, due to the steric repulsion of the triethylphosphines. No channels are observed in **7b** due to offset packing. The packing of **7c** is similar to that of **7a** (Figure 8).

Photophysical Properties. Upon formation, molecular rectangles **7a−c** assume an intense orange yellow color. The absorption spectrum of **7c** is shown in Figure 9. The absorbance in the electronic spectrum exhibits a near-UV transition, which is red-shifted relative to **2e** and very slightly blue-shifted relative to **6**. The absorbance per **2e** unit increases significantly upon

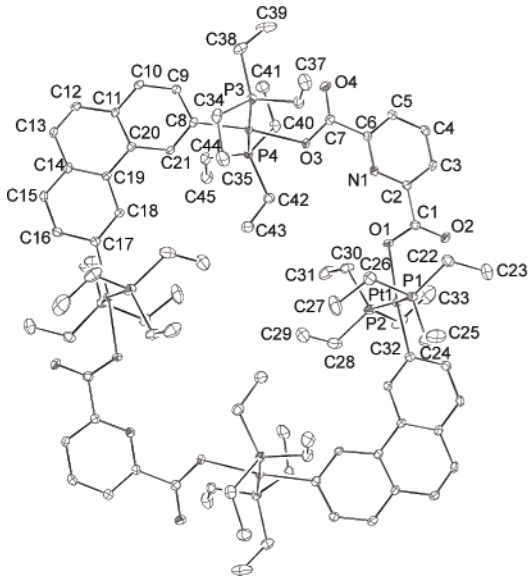

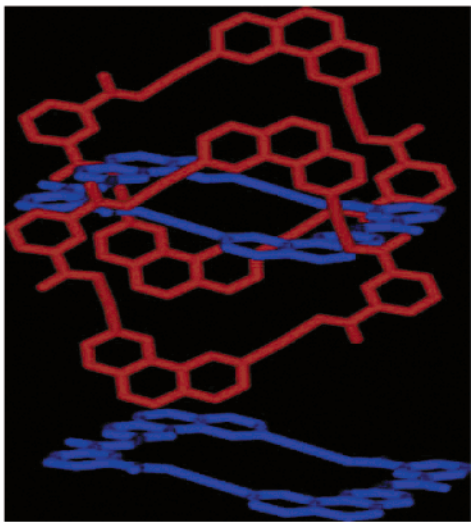

Figure 5. ORTEP presentation of **5b** with atom numbering (left). Packing nature of **5b**; triethylphosphine and solvent molecules are omitted for clarity (right).

Table 3. Crystallographic Data and Refinement Parameters for **7a**, **7b**, and **7c**

	7a	**7b**	**7c**
formula	$C_{90}H_{146}Cl_6P_8O_8Pt_4$	$C_{108}H_{156}Cl_{12}P_8O_8Pt_4$	$C_{107}H_{155}Cl_9N_4P_8O_8Pt_4$
fw	2596.89	3035.85	2972.52
temp (K)	150(1)	150(1)	150(1)
λ (Å)	0.71073	0.71073	0.71073
crystal system	triclinic	triclinic	triclinic
space group	$P\bar{1}$	$P\bar{1}$	$P\bar{1}$
a (Å)	12.293(2)	10.189(1)	10.237(3)
b (Å)	13.334(2)	17.496(4)	15.507(4)
c (Å)	18.456(3)	20.077(4)	21.718(7)
α (deg)	83.693(11)	65.803(9)	110.763(15)
β (deg)	82.697(9)	89.450(12)	92.454(21)
γ (deg)	63.396(10)	88.822(13)	102.612(18)
V (Å^3)	2678.43(7)	3264.21(10)	3118.72(16)
Z	1	1	1
D_{calc} (g/cm^3)	1.610	1.544	1.583
μ (mm^{-1})	5.523	4.663	4.818
F(000)	1284	1504	1474
reflns collected	19 399	22 753	22 242
unique reflns	12 195	14 832	14 021
max and min trans	0.5570, 0.2481	0.7067, 0.3885	0.7947, 0.2834
R1 [$I > 2\sigma(I)$][a]	0.0424	0.0847	0.0574
wR2	0.1032	0.2088	0.1065

[a] $R1 = (F_o - F_c)F_o$, $wR2 = [(w(F_o^2 - F_c^2)^2)/(F_o^2)^2]^{1/2}$.

Table 4. Selected Bond Lengths (Å) and Angles (deg) for Complexes **7a**−**c**

		7a			
Pt(1)−O(1)	2.117(4)	Pt(1)−P(2)	2.300(14)	Pt(1)−P(1)	2.304(14)
Pt(2)−O(3)	2.115(4)	Pt(2)−P(4)	2.296(15)	Pt(2)−P(3)	2.300(15)
O(1)−Pt(1)−P(2)	87.27(11)		O(1)−Pt(1)−P(1)	92.20(11)	
P(2)−Pt(1)−P(1)	178.68(5)		O(3)−Pt(2)−P(4)	88.53(13)	
O(3)−Pt(2)−P(3)	91.60(12)		P(4)−Pt(2)−P(3)	168.04(6)	
		7b			
Pt(1)−O(1)	2.122(8)	Pt(1)−P(2)	2.326(4)	Pt(1)−P(1)	2.295(4)
Pt(2)−O(3)	2.125(8)	Pt(2)−P(4)	2.304(3)	Pt(2)−P(3)	2.279(4)
O(1)−Pt(1)−P(2)	89.50(2)		O(1)−Pt(1)−P(1)	88.90(2)	
P(2)−Pt(1)−P(1)	175.49(17)		O(3)−Pt(2)−P(4)	91.70(3)	
O(3)−Pt(2)−P(3)	87.20(3)		P(4)−Pt(2)−P(3)	170.85(15)	
		7c			
Pt(1)−O(1)	2.131(5)	Pt(1)−P(2)	2.299(2)	Pt(1)−P(1)	2.317(2)
Pt(2)−O(3)	2.127(5)	Pt(2)−P(4)	2.286(2)	Pt(2)−P(3)	2.319(2)
O(1)−Pt(1)−P(2)	86.65(16)		O(1)−Pt(1)−P(1)	94.21(16)	
P(2)−Pt(1)−P(1)	169.22(9)		O(3)−Pt(2)−P(4)	85.01(17)	
O(3)−Pt(2)−P(3)	93.14(16)		P(4)−Pt(2)−P(3)	172.51(8)	

rectangle formation; likewise, the anthracene-based absorbance, centered around 280 nm, also increases significantly. In contrast, in the case of the analogous cationic rectangles, the anthracene-based absorbance decreased upon formation of a macrocycle.[2k]

Thermogravimetric Analysis. Single-crystal structure analysis of **3a**, **5a**, and **5b** reveals that solvent molecules are situated inside the macrocycles. However, **5a** readily loses solvent at ambient temperature. Thermogravimetric analysis (TGA) was performed on a polycrystalline sample of **3a** that showed a clean weight loss step in the temparature range of 58−127 °C, corresponding to the removal of nine guest water molecules in the cavities (calcd 4.36%, found 4.58%). However, no weight loss was observed between the temperature range of 130−210 °C, indicating that the guest-free compound was stable. Most significant is the fact that the TGA of the desolvated **3a** after being kept in the open atmosphere overnight showed a reversible uptake of water molecules. For complex **5b**, a weight loss was found in the temperature range of 107−120 °C, corresponding to the loss of two guest water molecules. In this case, the desolvation was found to be irreversible. The reversibility in the guest capturing behavior of **3a** is probably due to the presence of channels in the solid state.

Conclusion

The metal−oxygen coordination-driven self-assembly of neutral structures by combining Pt-containing units with anionic carboxylate linkers is a new method that enhances the scope of this branch of supramolecular chemistry. The formation of the nine new macrocycles described in this Article provides strong evidence in favor of the versatility of the chosen approach. These assemblies include previously unknown rectangles, triangles, and rhomboids, the structures of which have been determined

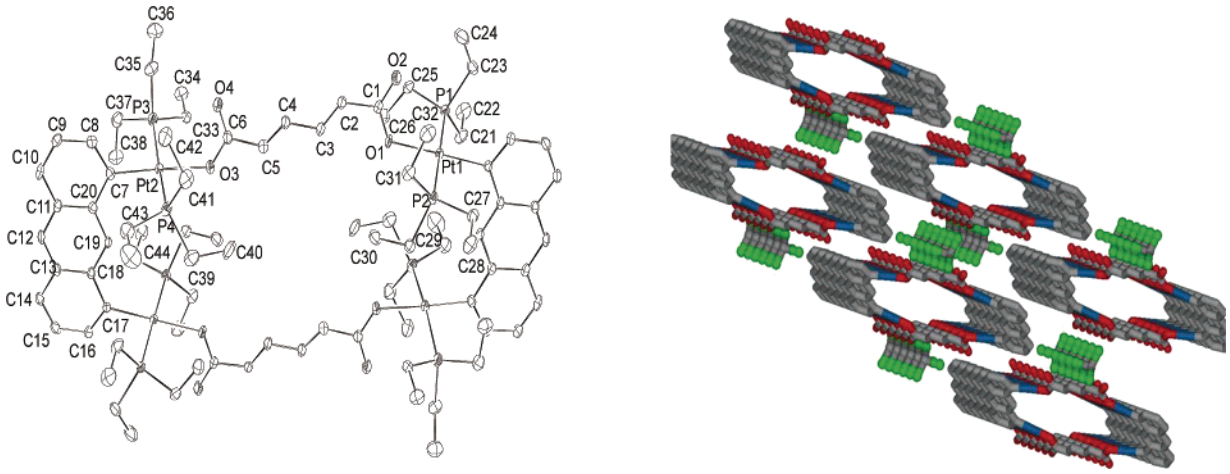

Figure 6. ORTEP presentation of **7a** with atom numbering (left). Packing diagram of **7a** along the *b* axis (right); solvent molecules are shown by ball-and-stick models (green balls are chlorine, gray balls are carbon).

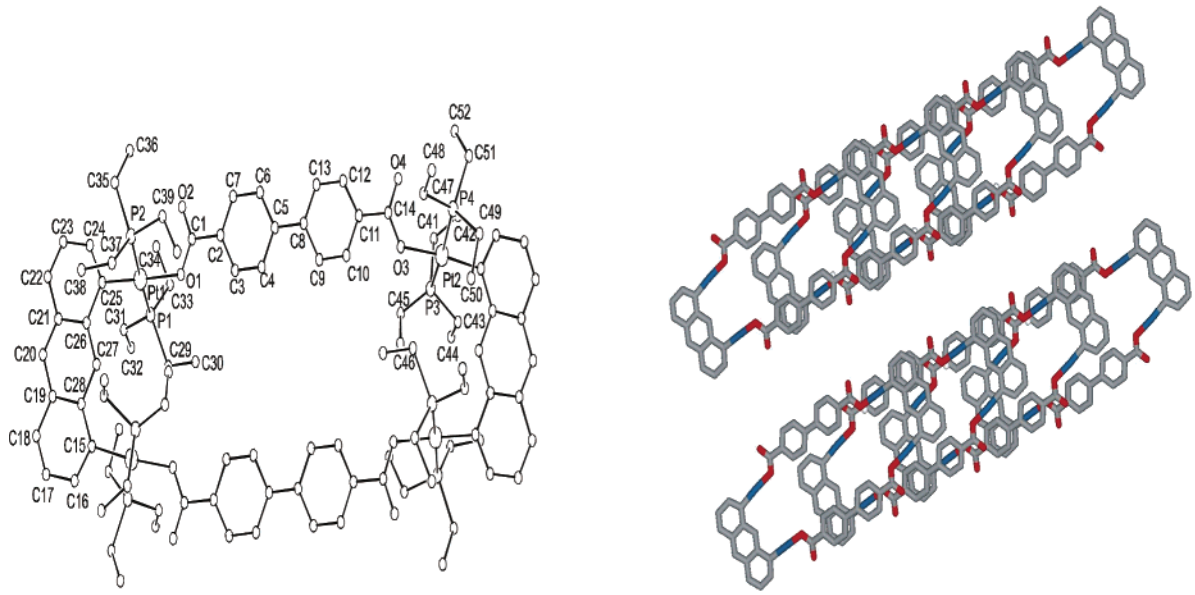

Figure 7. Molecular structure of **7b** with atom numbering (left). Packing diagram of **7b** is shown along the *a* axis; triethylphosphine and solvent molecules are omitted for clarity (right).

by NMR spectroscopy. In the case of triangles **3a** and **3b**, rhomboids **5a** and **5b**, and rectangles **7a**−**c**, the structures of the assemblies have been unambiguously established by X-ray crystallography. The crystallographic studies revealed in some cases the presence of different types of channels within the crystal lattice, which may be of importance for further studies into the properties of these new compounds.

Experimental Section

General Methods. Dicarboxylic acids (except *p*,*p*′-azodibenzoic acid) were purchased from Aldrich and used as received. The disodium salts of the acids were prepared by neutralizing the corresponding acids with $NaHCO_3$ in aqueous medium. The 2,9-bis[*trans*-Pt$(PEt_3)_2NO_3$]-phenanthrene **1**[4] and 1,8-bis[*trans*-Pt$(PEt_3)_2NO_3$]anthracene **6**[2k] were prepared according to known procedures. Deuterated solvents were purchased from Cambridge Isotope Laboratories. All NMR spectra were recorded on Varian Unity 300 or Varian XL-300 spectrometers. ^{1}H chemical shifts are reported relative to the residual protons of deuterated dichloromethane (δ 5.32 ppm) or relative to the residual protons of deuterated chloroform (δ 7.27 ppm). ^{31}P{H} chemical shifts are reported relative to an external, unlocked sample of H_3PO_4 (δ = 0.0 ppm). Elemental analyses were performed by Atlantic Microlab, Norcross, GA. IR spectra were recorded on a Nicolet 520 FTIR spectrometer in KBr pellets. UV−vis spectra were recorder on a Hewlett-Packard 8452A spectrophotometer. Thermogravimetric analysis (TGA) was performed on a TA Instruments TGA 2050 thermogravimetric analyzer under a flow of nitrogen (30 mL min^{-1}). The sample (particle size 50−200 mesh) was heated at a rate of 10 °C min^{-1} with inert alumina as a reference.

X-ray Data Collection, Structure Solution, and Refinement. A single crystal of the corresponding complex (**3a**,**b**, **5a**,**b**, **7a**−**c**) was selected from the reaction product and was mounted on a glass fiber with traces of viscous oil and then transferred to a Nonius KappaCCD diffractometer equipped with Mo Kα radiation (λ = 0.71073 Å). Ten frames of data were collected at 150(1) K with an oscillation range of 1 deg/frame and an exposure time of 20 s/frame.[16] Indexing and unit cell refinement were based on all of the observed reflections from those 10 frames. Structures were solved by a combination of direct methods and heavy atom using SIR 97.[17] All of the non-hydrogen atoms were

(16) COLLECT Data Collection Software. Nonius B. V. 1998.

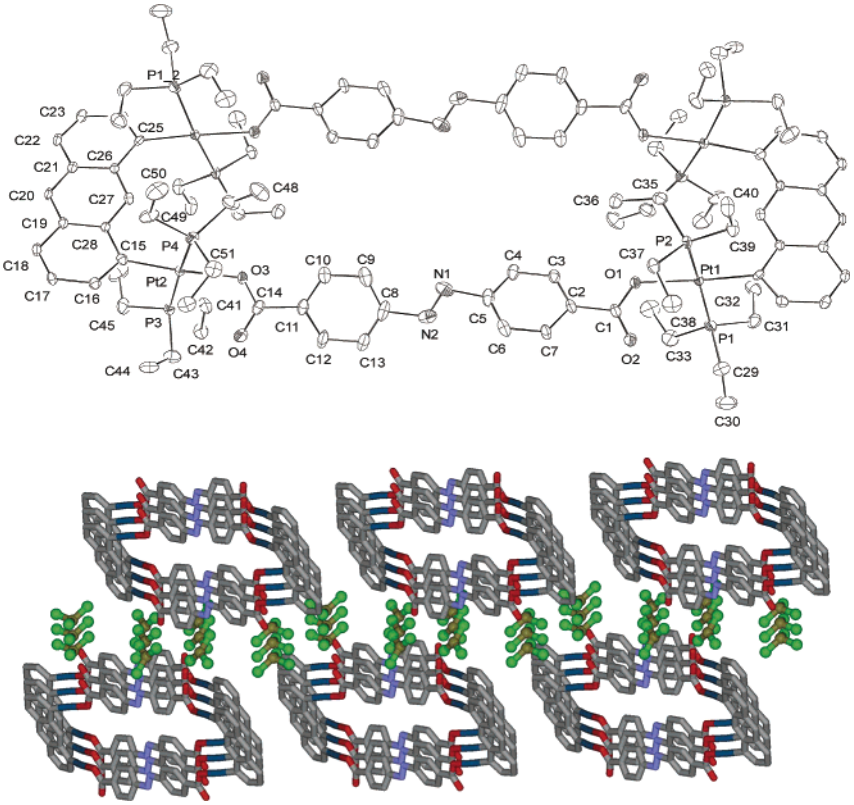

Figure 8. ORTEP presentation of **7c** with atom numbering (top) (ellipsoids are drawn at 30% probability). Packing diagram; solvents ($CHCl_3$) are shown as ball-and-stick models (bottom).

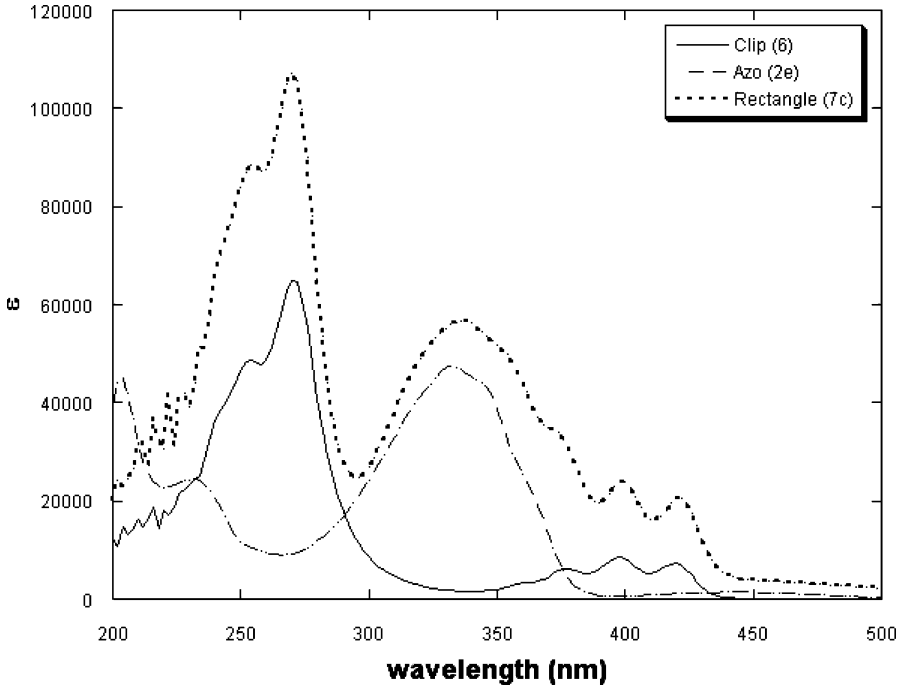

Figure 9. Absorption spectra of supramolecular rectangle **7c** (10 μM) and building blocks **6** (20 μM) and **2e** (20 μM).

refined with anisotropic displacement coefficients. Hydrogen atoms were assigned isotropic displacement coefficients $U(H) = 1.2U(C)$ or $1.5U$(C-methyl), and their coordinates were allowed to ride on their respective carbons using SHELXL97.[18] Scattering factors were taken from the International Table of Crystallography, Vol. C.[19,20] The weighting scheme employed was $w = 1/[\sigma^2(F_o^2) + (0.0253P)^2 + 18.4225P]$, where $P = (F_o^2 + 2F_c^2)/3$. Structure solution of **7b** showed high disorder and a high *R* factor. Details of the data collection, structure

(17) Altomare, A.; Burla, M. C.; Camalli, M.; Cascarano, G.; Giacovazzo, C.; Guagliardi, A.; Moliteni, A. G. G.; Polidori, G.; Spagna, R. SIR97 (Release 1.02): A program for automatic solution and refinement of crystal structure.

(18) SHELX97 [Includes SHELXS97, SHELXL97, CIFTAB] − Sheldrick, G. M. 1997. Programs for Crystal Structure Analysis (Release 97−2). University of Göttingen, Germany.

solution, and refinement are given in Table 1 (for **3a**, **3b**, **5a**, **5b**) and Table 3 (for **7a**−**c**).

Synthesis of [NaOOC−C_6H_4N═NC_6H_4−COONa] (2e). An aqueous solution (100 mL) of sodium hydroxide (12 g) and 4-nitrobenzoic acid (7.0 g) was heated on a water bath (70 °C). A hot aqueous solution of glucose (60% w/v) was then added slowly at 70 °C, whereupon a yellow precipitate formed which immediately turned brown upon further addition of the glucose solution. The mixture was kept in a refrigerator overnight, and a light brown precipitate was obtained. This was filtered, washed with cold water, and then dissolved in hot water. Acetic acid was added to acidify, whereupon a light red precipitate was obtained. This was filtered, washed with water (100 mL), and dried in an oven at 100 °C (yield 5 g). This acid was neutralized with an equivalent amount of $NaHCO_3$ at ambient temperature to produce the disodium salt. ^{1}H NMR (CD_3Cl, 300 MHz): 8.30 (d, 4H), 8.00 (d, 4H).

General Procedure for the Preparation of Compounds 3a−c. To a 4 mL acetone solution containing 11.62 mg (0.010 mmol) of nitrate **1** was added an aqueous solution (4 mL) of disodium salt (0.010 mmol) of the appropriate acid (**2a**−**c**) drop by drop with continuous stirring (10 min), whereupon the colorless product precipitated. This was centrifuged and washed several times with acetone and water and was dried in an oven at 80 °C. The colorless powder was redissolved in a 1:1 mixture of chloroform/dichloromethane (1.5 mL). Colorless platelike single crystals suitable for X-ray diffraction were obtained by diffusing acetone into this solution. For **3d**, only a very small amount of precipitate formed after mixing the components, so the mixture was stirred for an extra 2 h to obtain the product in high yield.

Cyclotris[(2,9-bis[*trans*-Pt(PEt_3)$_2$]phenanthrene)(*trans*,*trans*-OOC−$(CH)_4$−COO)] (3a). Yield (97.9%). Anal. Calcd for $C_{132}H_{216}O_{12}P_{12}Pt_6$·$9H_2O$: C, 42.80; H, 6.32. Found: C, 42.45; H, 6.42. ^{31}P{^{1}H} NMR ($CDCl_3$, 121.4 MHz): δ 17.47 (s, $^1J_{PPt}$ = 2879.8 Hz). ^{1}H NMR (CD_3Cl, 300 MHz): 8.64 (s, 6H, H_1), 7.67 (d, 6H, $^3J_{H4-H3}$ = 8.3 Hz, H_3), 7.43 (s, 6H, H_5), 7.38 (d, 6H, $^3J_{H4-H3}$ = 8.1 Hz, H_4), 7.12 (dd, 6H, $^3J_{HaHb}$ = 11.40 Hz, $^3J_{HaHb'}$ = 3.00 Hz H_a-muconate), 6.21 (dd, 6H, $^3J_{HbHa}$ = 11.40 Hz, $^3J_{HbHa'}$ = 3.00 Hz, H_b-muconate), 1.50 (m, 72H, PCH_2CH_3), 1.15 (m, 108H, PCH_2CH_3). IR: ν(COO$^-$), 1638, 1592 cm^{-1}; ν(O−H), 3200−3350 cm^{-1}.

Cyclotris[(2,9-bis[*trans*-Pt(PEt_3)$_2$]phenanthrene)(1,4-OOC−C_6H_4−COO)] (3b). Yield (98.6%). Anal. Calcd for $C_{138}H_{216}O_{12}P_{12}Pt_6$·$2CHCl_3$: C, 43.65; H, 5.66. Found: C, 43.51; H, 5.47. ^{31}P{^{1}H} NMR ($CDCl_3$, 121.4 MHz): δ 17.62 (s, $^1J_{PPt}$ = 2879.8 Hz). ^{1}H NMR (CD_3Cl, 300 MHz): 8.73 (s, 6H, H_1), 8.07 (s, 12H, H-terephthalate), 7.72 (d, 6H, $^3J_{H4-H3}$ = 8.3 Hz, H_3), 7.46 (s, 6H, H_5), 7.41 (d, 6H, $^3J_{H4-H3}$ = 8.1 Hz, H_4), 1.50 (m, 72H, PCH_2CH_3), 1.20 (m, 108H, PCH_2CH_3). IR: ν (COO$^-$), 1639, 1572 cm^{-1}.

Cyclotris[(2,9-bis[*trans*-Pt(PEt_3)$_2$]phenanthrene)(4,4′-OOC−C_6H_4−C_6H_4−COO)] (3c). Yield (98.8%). Anal. Calcd for $C_{156}H_{228}O_{12}P_{12}Pt_6$: C, 48.81; H, 5.94. Found: C, 48.43; H, 5.77. ^{31}P{^{1}H} NMR ($CDCl_3$, 121.4 MHz): δ 17.46 (s, $^1J_{PPt}$ = 2818.8 Hz). ^{1}H NMR ($CDCl_3$, 300 MHz): 8.68 (s, 6H, H_1), 8.17 (d, 12H, H-biphenyl), 7.72 (d, 6H, $^3J_{H4-H3}$ = 8.05 Hz, H_3), 7.68 (d, 12H, biphenyl), 7.47 (s, 6H, H_5), 7.40 (d, 6H, $^3J_{H4-H3}$ = 8.06 Hz, H_4), 1.54 (m, 72H, PCH_2CH_3), 1.14 (m, 108H, PCH_2CH_3). IR: ν (COO$^-$), 1619, 1593 cm^{-1}.

Cyclotris[(2,9-bis[*trans*-Pt(PEt_3)$_2$]phenanthrene)(1,4-OCC−CHCH−C_6H_4−CHCH−COO)] (3d). Yield (97.2%). Anal. Calcd for $C_{150}H_{228}O_{12}P_{12}Pt_6$: C, 47.84; H, 6.06. Found: C, 47.63; H, 5.97. ^{31}P-{^{1}H} NMR (CD_2Cl_2, 121.4 MHz): δ 17.55 (s, $^1J_{PPt}$ = 2897.52 Hz). ^{1}H NMR (CD_2Cl_2, 300 MHz): 8.66 (s, 6H, H_1), 7.69 (d, 6H, $^3J_{H4-H3}$ = 8.15 Hz, H_3), 7.58 (s, 12H, phenyl of **2d**), 7.44 (s, 6H, H_5), 7.40 (t, 6H, $^3J_{H4-H3}$ = 8.06 Hz, H_4), 6.66 (s, 6H, ethylenic H of **2d**), 6.60 (s, 6H, ethylenic H of **2d**), 1.60 (m, 72H, PCH_2CH_3), 1.20 (m, 108H, PCH_2CH_3). IR: ν (COO$^-$), 1638, 1592 cm^{-1}.

General Procedure for the Preparation of Compounds 5a,b. Rhomboids were obtained as a white precipitate by reacting 11.62 mg of nitrate **1** (0.01 mmol) and 120° rigid linker (**4a** or **4b**) in a 1:1 stoichiometric ratio, applying the same synthetic procedure as mentioned for **3a**−**c**. Colorless single crystals of **5a** for X-ray structure analysis were grown overnight by diffusion of acetone into the chloroform/dichloromethane mixture solution of the product. For **5b**, crystals were obtained after 2 weeks of diffusion of acetone into a chloroform/nitromethane solution of the product.

Cyclobis[(2,9-bis[*trans*-Pt(PEt_3)$_2$]phenanthrene)(1,3-OOC−C_6H_4−COO)] (5a). Yield (98.6%). Anal. Calcd for $C_{92}H_{144}O_8P_8Pt_4$: C, 45.92; H, 5.99. Found: C, 45.63; H, 6.17. ^{31}P{^{1}H} NMR ($CDCl_3$, 121.4 MHz): δ 17.52 (s, $^1J_{PPt}$ = 2879.8 Hz). ^{1}H NMR ($CDCl_3$, 300 MHz): 8.72 (s, 4H, H_1), 8.64 (t, 2H, H_2-isophthalate), 8.12 (dd, 6H, H-isophthalate), 7.77 (d, 4H, $^3J_{H4-H3}$ = 8.3 Hz, H_3), 7.47 (s, 4H, H_5), 7.43 (d, 4H, $^3J_{H4-H3}$ = 8.1 Hz, H_4), 1.55 (m, 48H, PCH_2CH_3), 1.40 (m, 72H, PCH_2CH_3). IR: ν (COO$^-$), 1619, 1570 cm^{-1}.

Cyclobis[(2,9-bis[*trans*-Pt(PEt_3)$_2$]phenanthrene)(2,6-OOC−Py−COO)] (5b). Yield (98.8%). Anal. Calcd for $C_{90}H_{142}O_8N_2P_8Pt_4$·$2H_2O$: C, 44.22; H, 5.97; N, 1.14. Found: C, 44.53; H, 5.87; N, 0.99. ^{31}P-{^{1}H} NMR ($CDCl_3$, 121.4 MHz): δ 17.14 (s, $^1J_{PPt}$ = 2899.95 Hz). ^{1}H NMR ($CDCl_3$, 300 MHz): 8.63 (s, 4H, H_1), 8.17 (d, 6H, $^3J_{H4-H3}$ = 7.80 Hz, phenyl of **2d**), 7.75 (dd, 4H, H_3), 7.47 (s, 4H, H_5), 7.39 (d, 4H, $^3J_{H4-H3}$ = 8.06 Hz, H_4), 1.54 (m, 72H, PCH_2CH_3), 1.15 (m, 108H, PCH_2CH_3). IR: ν(COO$^-$), 1633, 1572 cm^{-1}; ν(O−H), 3240−3360 cm^{-1}.

General Procedure for the Preparation of Compounds 7a−c. To a 3 mL acetone solution containing 11.62 mg (0.010 mmol) of 1,8-bis(*trans*-Pt(PEt_3)$_2$(NO_3))anthracene **6** was added an aqueous solution (3 mL) of the disodium salt of the appropriate acid (**2a**, **2c**, or **2e**) (0.010 mmol) drop by drop with continuous stirring (15 min). The orange yellow products, which precipitated, were filtered and washed with acetone. For **7a**, the reaction mixture was stirred overnight before self-assembly was complete. Orange yellow platelike single crystals for structure analysis were obtained overnight by vapor diffusion of acetone into the chloroform/dichloroform solution of the product.

Cyclobis[(1,8-bis[*trans*-Pt(PEt_3)$_2$]anthracene)(*trans*,*trans*-OOC−$(CH)_4$−COO)] (7a). Yield (97.4%). Anal. Calcd for $C_{88}H_{144}O_8P_8Pt_4$·$2CHCl_3$: C, 41.58; H, 5.62. Found: C, 41.83; H, 5.97. ^{31}P{^{1}H} NMR ($CDCl_3$, 121.4 MHz): δ 12.84 (s, $^1J_{PPt}$ = 2874 Hz). ^{1}H NMR (CD_3Cl, 300 MHz): δ 9.58 (s, 2H, H_9), 8.16 (s, 2H, H_{10}), 7.64 (d, 4H, $^3J_{HH}$ = 6.84 Hz, $H_{4,5}$), 7.53 (d, 4H, $^3J_{HH}$ = 8.55 Hz, $H_{2,7}$), 7.18 (dd, 4H, $^3J_{HaHb}$ = 2.89 Hz, $^3J_{HaHb'}$ = 2.68 Hz, H_a-muconate), 6.97 (t, 4H, $H_{3,6}$), 6.20 (dd, 4H, $^3J_{HbHa}$ = 2.89 Hz, $^3J_{HbHa'}$ = 2.68 Hz, H_b-muconate), 1.57 (m, 48H, PCH_2CH_3), 1.01 (m, 72H, PCH_2CH_3). IR: ν(COO$^-$), 1613, 1570 cm^{-1}.

Cyclobis[(1,8-bis[*trans*-Pt(PEt_3)$_2$]anthracene)(4,4′-OOC−C_6H_4−C_6H_4−COO)] (7b). Yield (98.0%). Anal. Calcd for $C_{104}H_{152}O_8P_8Pt_4$·$4CHCl_3$: C, 42.68; H, 5.13. Found: C, 42.43; H, 5.27. ^{31}P{^{1}H} NMR ($CDCl_3$, 121.4 MHz): δ 13.31 (s, $^1J_{PPt}$ = 2876 Hz). ^{1}H NMR (CD_3Cl, 300 MHz): δ 9.75 (s, 2H, H_9), 8.29 (m, 10H, H_{10}, H_α-biphenyl), 7.70 (m, 12H, H_β-biphenyl, $H_{4,5}$), 7.56 (d, 4H, $^3J_{HH}$ = 8.30 Hz, $H_{2,7}$), 7.02 (t, 4H, $H_{3,6}$), 1.58 (m, 48H, PCH_2CH_3), 1.05 (m, 72H, PCH_2CH_3). IR: ν(COO$^-$), 1619, 1593 cm^{-1}.

Cyclobis[(1,8-bis[*trans*-Pt(PEt_3)$_2$]anthracene)(4,4′-OOC−C_6H_4N═NC_6H_4−COO)] (7c). Yield (98.7%). Anal. Calcd for $C_{104}H_{152}O_8N_4P_8Pt_4$·$3CHCl_3$: C, 43.19; H, 5.21; N, 1.88. Found: C, 43.33; H, 5.11; N, 1.98. ^{31}P{^{1}H} NMR ($CDCl_3$, 121.4 MHz): δ 13.36 (s, $^1J_{PPt}$ = 2876 Hz). ^{1}H NMR (CD_3Cl, 300 MHz): δ 9.68 (s, 2H, H_9), 8.29 (d, 8H, $^3J_{HH}$ = 8.51 Hz, H_α-azobiphenyl), 8.20 (s, 2H, H_{10}), 8.00 (d, 8H, $^3J_{HH}$ = 8.44 Hz, H_β-azobiphenyl), 7.20 (d, 4H, $^3J_{HH}$ = 6.7 Hz, $H_{4,5}$), 7.57

(19) Maslen, E. N.; Fox, A. G.; O'Keefe, M. A. In *International Tables for Crystallography: Mathemetical, Physical and Chemical Tables*; Wilson, A. J. C., Ed.; Kluwer: Dordrecht, The Netherlands, 1992; Vol. C, Chapter 6, pp 476−516.
(20) Creagh, D. C.; McdAuley, W. J. In *International Tables for Crystallography: Mathematical, Physical and Chemical Tables*; Wilson, A. J. C., Ed.; Kluwer: Dordrecht, The Netherlands, 1992; Vol. C, Chapter 4, pp 206−222.

(d, 4H, $^3J_{HH}$ = 8.38 Hz, $H_{2,7}$), 7.02 (t, 4H, $H_{3,6}$), 1.58 (m, 48H, PCH_2CH_3), 1.05 (m, 72H, PCH_2CH_3). IR: $\nu(COO^-)$, 1629, 1583 cm^{-1}.

Acknowledgment. Financial support by the NSF (CHE-0306720) and the NIH (GM-57052) is gratefully acknowledged. We thank Mr. Kendrick Nelson for technical assistance with the absorption spectra.

Supporting Information Available: ^{31}P and ^1H NMR spectra of all of the macrocycles (PDF), crystallographic files (in CIF format) of **3a**−**b**, **5a**−**b**, and **7a**−**c**. This material is available free of charge via the Internet at http://pubs.acs.org.

JA039235B